ARS MATHEMATICA CONTEMPORANEA

ISSN 1855-3966 (printed edn.), ISSN 1855-3974 (electronic edn.)
ARS MATHEMATICA CONTEMPORANEA 22 (2022) #P4.07 / 617–636
https://doi.org/10.26493/1855-3974.2740.7ab
(Also available at http://amc-journal.eu)

S^2 coverings by isosceles and scalene triangles – adjacency case II*

Catarina P. Avelino [†]

Center of Mathematics of the University of Minho – UTAD Pole (CMAT-UTAD), University of Trás-os-Montes e Alto Douro, Vila Real, Portugal and *Center for Computational and Stochastic Mathematics (CEMAT), University of Lisbon (IST-UL), Portugal*

Altino F. Santos

Center of Mathematics of the University of Minho – UTAD Pole (CMAT-UTAD), University of Trás-os-Montes e Alto Douro, Vila Real, Portugal

Received 4 April 2019, accepted 6 January 2022, published online 11 August 2022

Abstract

The aim of this paper is to complete the study and classification of spherical f-tilings by scalene triangles T and isosceles triangles T' within a subclass defined by the adjacency of the lower side of T and the longest side of T'. It consists of eight families of f-tilings (two families with one continuous parameter, one family with one discrete parameter and one continuous parameter, and five families with one discrete parameter). We also analyze the combinatorial structure of all these families of f-tilings, as well as the group of symmetries of each tiling; the transitivity classes of isogonality are included.

Keywords: Dihedral f-tilings, combinatorial properties, spherical trigonometry.

Math. Subj. Class. (2020): 52C20, 52B05, 20B35

*This research was partially financed by Portuguese Funds through FCT (Fundação para a Ciência e a Tecnologia) within the projects UIDB/00013/2020 and UIDP/00013/2020 of CMAT-UTAD, Center of Mathematics of University of Minho, and projects UIDB/04621/2020 and UIDP/04621/2020 of CEMAT/IST-ID, Center for Computational and Stochastic Mathematics, Instituto Superior Técnico, University of Lisbon.

[†]Corresponding author.

E-mail addresses: cavelino@utad.pt (Catarina P. Avelino), afolgado@utad.pt (Altino F. Santos)

1 Introduction

A *folding tessellation* or *folding tiling* (f-tiling, for short) of the sphere S^2 is an edge-to-edge finite polygonal tiling τ of S^2 such that all vertices of τ satisfy the angle-folding relation, i.e., each vertex is of even valency and the sums of alternating angles around each vertex are equal to π.

F-tilings are intrinsically related to the theory of isometric foldings of Riemannian manifolds, introduced by Robertson [10] in 1977. In several situations (beyond the scope of this paper), the edge-complex associated to a spherical f-tiling is the set of singularities of some spherical isometric folding.

The classification of f-tilings was initiated by Breda [2], with a complete classification of all spherical monohedral (triangular) f-tilings. Afterwards, in 2002, Ueno and Agaoka [11] have established the complete classification of all triangular monohedral tilings of the sphere (without any restrictions on angles). Curiously, the triangular tilings of even valency at any vertex are necessarily f-tilings. Dawson has also been interested in special classes of spherical tilings, see [3, 4, 5], for instance. Spherical f-tilings by two noncongruent classes of isosceles triangles have recently been obtained [6, 7].

The study of dihedral triangular f-tilings involving scalene triangles is clearly more unwieldy and was initiated in [1]. In this paper we complete the classification of spherical f-tilings by scalene triangles T and isosceles triangles T' resulting from the adjacency of the lower side of T and the longest side of T'.

From now on,

(i) T denotes a spherical scalene triangle with internal angles $\alpha > \beta > \gamma$ and side lengths $a > b > c$;

(ii) T' denotes a spherical isosceles triangle with internal angles $(\delta, \delta, \varepsilon)$, $\delta \neq \varepsilon$, and side lengths (d, d, e),

as illustrated in Figure 1.

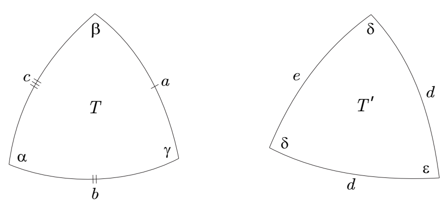

Figure 1: A spherical scalene triangle, T, and a spherical isosceles triangle, T'.

We shall denote by $\Omega(T, T')$ the set, up to isomorphism, of all dihedral folding tilings of S^2 whose prototiles are T and T' in which the lower side of T is equal to the longest side T'.

Taking into account the area of the prototiles T and T', we have

$$\alpha + \beta + \gamma > \pi \quad \text{and} \quad 2\delta + \varepsilon > \pi.$$

As $\alpha > \beta > \gamma$, we also have $\alpha > \frac{\pi}{3}$. In [8] it was established that any $\tau \in \Omega(T, T')$ has necessarily vertices of valency four.

We begin by pointing out that any element of $\Omega\,(T, T')$ has at least two cells congruent to T and T', respectively, such that they are in adjacent positions and in one and only one of the situations illustrated in Figure 2.

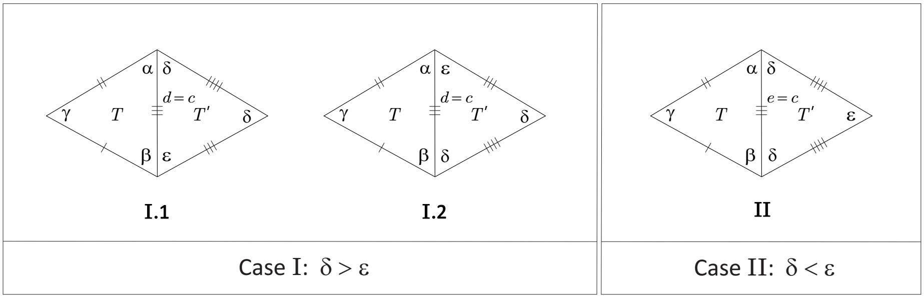

Figure 2: Distinct cases of adjacency.

In this paper we will consider the second case of adjacency. The next section contains the main result of this paper. In Section 2 we describe the eight families of spherical f-tilings that we may obtain from the second case of adjacency (Figure 2-II). The combinatorial structure of these tilings, the classification of the group of symmetries and also the transitivity classes of isogonality are presented. The proof of the main result consists of a long and exhaustive method and it is presented in Section 3.

2 Main result - Elements of $\Omega\,(T, T')$ in the case of Adjacency II

Theorem 2.1. *Let T and T' be a spherical scalene triangle and a spherical isosceles triangle, respectively, such that they are in adjacent positions as illustrated in* Figure 2-II. *Within this case, the f-tilings of $\Omega\,(T, T')$ are*

$$\mathcal{L}_\beta,\quad \mathcal{D}^k_\varepsilon\ (k \geq 4),\quad \mathcal{M}_\gamma,\quad \mathcal{N}^k\ (k \geq 6),\quad \mathcal{P}^k\ (k \geq 3),\quad \mathcal{Q}^k\ (k \geq 4),\quad \mathcal{R}^k\ (k \geq 6)\quad \text{and}\quad \mathcal{S}^k\ (k \geq 7),$$

that satisfy, respectively:

(i) $\alpha + \delta + \beta = \pi,\ \varepsilon = \frac{\pi}{2},\ \gamma = \frac{\pi}{3}$, *where α and β satisfy*

$$\sin^2(\alpha + \beta)\,(1 + 2\cos(\alpha - \beta)) = 2 \sin\alpha \sin\beta \quad \text{and} \quad \beta \in \left(\frac{\pi}{3}, \arccos\frac{\sqrt{6}}{6}\right);$$

(ii) $\alpha + \delta = \pi,\ \delta + \beta + \varepsilon = \pi,\ k\gamma = \pi,\ \delta = \delta^1_k(\varepsilon),\ \varepsilon \in \left(\varepsilon_{\min}, \frac{(k-1)\pi}{k}\right), k \geq 4,$

$$\text{where}\quad \delta^1_k(\varepsilon) = \arctan\frac{2\sin\varepsilon\cos^2\frac{\varepsilon}{2}}{\cos\frac{\pi}{k} - \cos^2\varepsilon} \quad \text{and} \quad \varepsilon_{\min} = \arccos\frac{\sqrt{1 + 8\cos\frac{\pi}{k}} - 1}{4};$$

(iii) $\alpha + \delta = \pi,\ \varepsilon = \frac{\pi}{2},\ \beta + \delta + \gamma = \pi,\ \delta = \gamma$ *and* $\gamma \in \left(\frac{\pi}{4}, \frac{\pi}{3}\right)$;

(iv) $\alpha + \delta = \pi,\ \varepsilon = \frac{\pi}{2},\ \beta + 3\delta = \pi,\ k\gamma = \pi$ *and* $\delta = \delta_k^2 = \arccos \sqrt{\frac{1}{2} \cos \frac{\pi}{k}},\ k \geq 6$;

(v) $\alpha + \delta = \pi,\ \varepsilon = \frac{\pi}{2},\ 2\beta + 2\delta = \pi,\ \beta + \delta + k\gamma = \pi$ *and* $\delta = \delta_k^3 = \arctan\left(\sec \frac{\pi}{2k}\right)$, $k \geq 3$;

(vi) $\alpha + \delta = \pi,\ \varepsilon = \frac{\pi}{2},\ 2\beta + 2\delta + \gamma = \pi,\ \beta + \delta + k\gamma = \pi,\ \delta = \delta_k^4,\ k \geq 4$, *where*

$$\delta_k^4 = \arctan\left(\sin \frac{(k-1)\pi}{2k-1} \sec \frac{\pi}{2k-1}\right);$$

(vii) $\alpha + \delta = \pi,\ \varepsilon = \frac{\pi}{2},\ 2\beta + 2\delta = \pi,\ k\gamma = \pi$ *and* $\alpha = \alpha_k^2 = 2\arctan(\cos \frac{\pi}{k} + \sqrt{1 + \cos^2 \frac{\pi}{k}}),\ k \geq 6$;

(viii) $\alpha + \delta = \pi,\ \varepsilon = \frac{\pi}{2},\ 2\beta + 2\delta + \gamma = \pi,\ k\gamma = \pi$ *and* $\delta = \delta_k^5,\ k \geq 7$, *where*

$$\delta_k^5 = \arctan\left(\sin \frac{(k-1)\pi}{2k} \sec \frac{\pi}{k}\right).$$

For each family of f-tilings we present the distinct classes of congruent vertices in Figure 3 (including the respective number of vertices in each tiling).

Particularizing suitable values for the parameters involved in each case, the corresponding 3D representations of these families of f-tilings are given in Figure 4. In each case, we present two perspectives in order to provide a more effective visualization of each f-tiling's combinatorial structure. Regarding the f-tiling P^k, $k \geq 3$, it can be observed that, if we consider the great circle that contains the four vertices surrounded by $(\beta, \delta, \delta, \beta, \gamma, \gamma, ..., \gamma)$ (marked in red) as the equator line and rotating the southern hemisphere 90 degrees (around the "vertical" axis) we obtain the f-tiling R^{2k}. Also, it is interesting to relate the monohedral edge-to-edge tilings TI_{16n+8} and I_{8n} described by Ueno and Agaoka in [11] with the families of f-tilings Q^k, $k \geq 4$, and S^k, $k \geq 7$, obtained by subdividing the prototypes in the monohedral tilings into two triangles satisfying the conditions of Figure 2-II. Seeing from another perspective, we obtain TI_{16n+8} and I_{8n} eliminating the vertices surrounded by $(\alpha, \alpha, \delta, \delta)$ (marked in green) and two suitable edges emanating from those vertices of Q^k, $k \geq 4$, and S^k, $k \geq 7$, respectively.

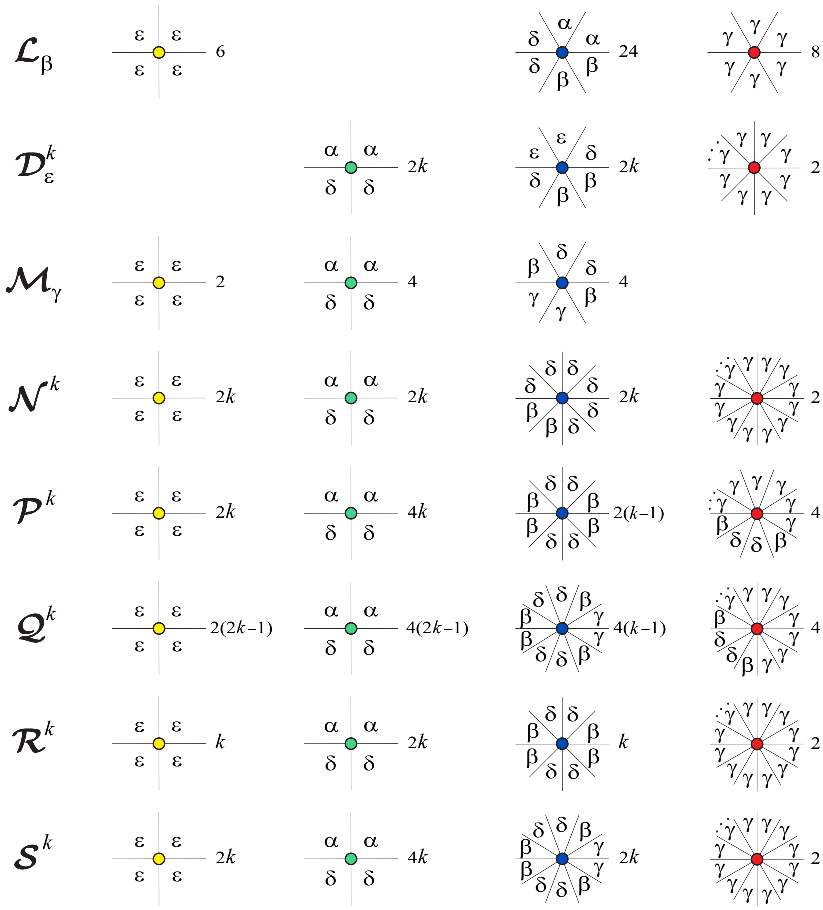

Figure 3: Distinct classes of congruent vertices.

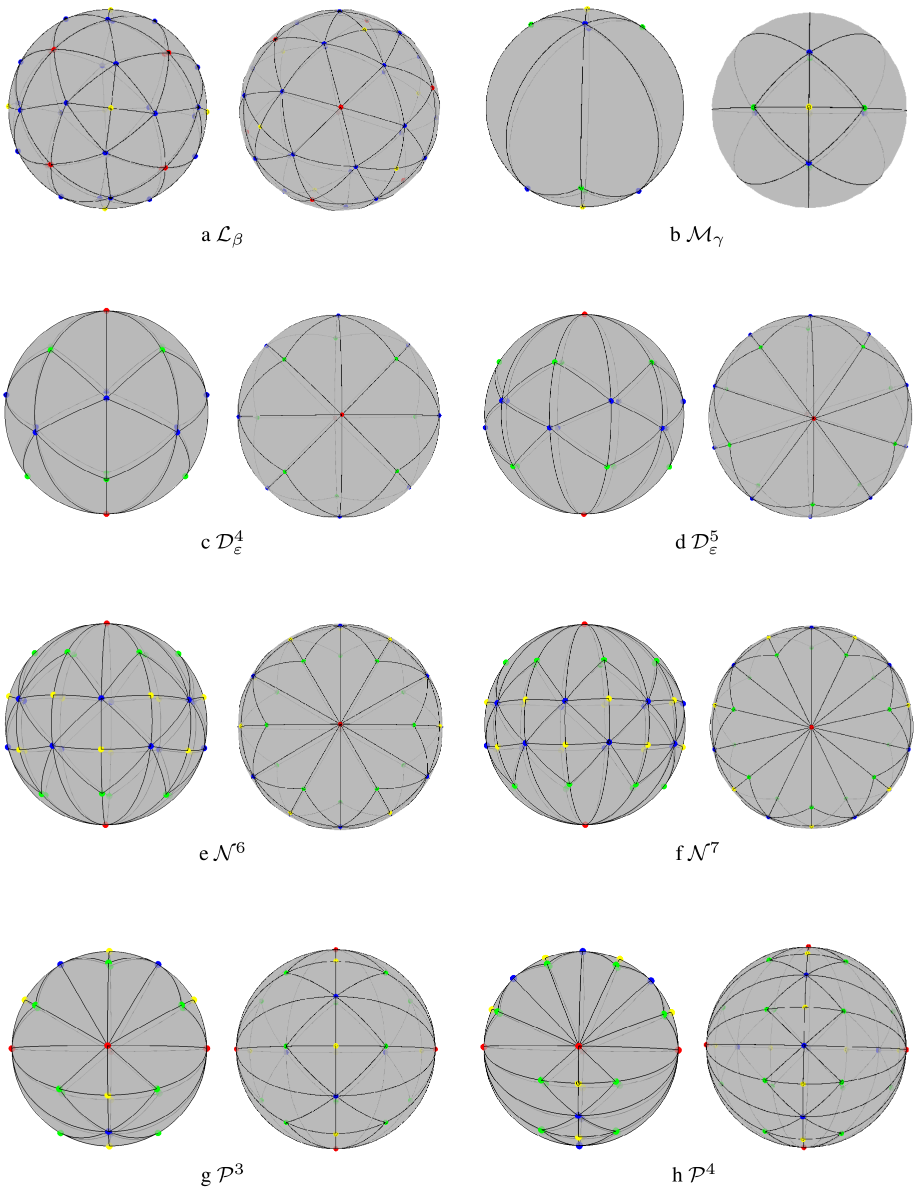

Figure 4: Elements of $\Omega(T, T')$ in the case of adjacency II.

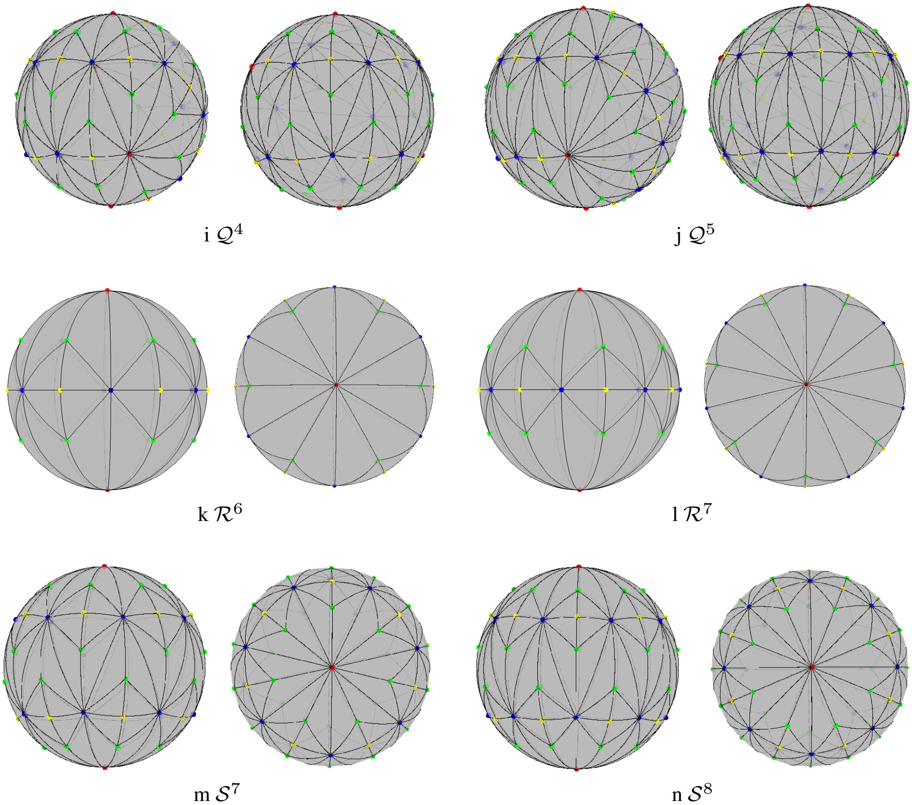

Figure 4: Elements of $\Omega(T, T')$ in the case of adjacency II.

The combinatorial structure of the classes of spherical f-tilings mentioned in Theorem 2.1, including the symmetry groups, is summarized in Table 1 (the analysis of the symmetry groups is similar to that applied in previous articles, *e.g.* [9]). Our notation is as follows:

- $|V|$ is the number of distinct classes of congruent vertices;
- N_1 and N_2 are, respectively, the number of triangles congruent to T and T', respectively;
- $G(\tau)$ is the symmetry group of each tiling $\tau \in \Omega(T, T')$ and the index of isogonality for the symmetry group is denoted by #isog.;
- C_n is the cyclic group of order n;
- $V \simeq C_2 \times C_2$ is the Klein group;
- D_n is the n^{th} dihedral group (it consists of n rotations and n reflections);
- O is the chiral group with 24 elements;

- $i(k) = \begin{cases} \frac{3k}{2} + 1 & \text{if } k \text{ even} \\ \frac{3k+1}{2} + 1 & \text{if } k \text{ odd.} \end{cases}$

f-tiling	α	β	γ	δ	ε	$\|V\|$	N_1	N_2	$G(\tau)$	#isog.
$\mathcal{L}_\beta$	$\alpha(\beta)$	$\left(\frac{\pi}{3}, \arccos\frac{\sqrt{6}}{6}\right)$	$\frac{\pi}{3}$	$\pi-\alpha-\beta$	$\frac{\pi}{2}$	3	48	24	O	3
$\mathcal{D}^k_\varepsilon$, $k \geq 4$	$\pi-\delta$	$\pi-\delta-\varepsilon$	$\frac{\pi}{k}$	$\delta^1_k(\varepsilon)$	$(\varepsilon_{\min}, \varepsilon_{\max})$	3	$4k$	$4k$	D_{2k}	3
$\mathcal{M}_\gamma$	$\pi-\gamma$	$\pi-2\gamma$	$\left(\frac{\pi}{4}, \frac{\pi}{3}\right)$	γ	$\frac{\pi}{2}$	3	8	8	V	3
$\mathcal{N}^k$, $k \geq 6$	$\pi-\delta$	$\pi-3\delta$	$\frac{\pi}{k}$	δ^2_k	$\frac{\pi}{2}$	4	$4k$	$8k$	D_{2k}	4
$\mathcal{P}^k$, $k \geq 3$	$\pi-\delta$	$\frac{\pi}{2}-\delta$	$\frac{\pi}{2k}$	δ^3_k	$\frac{\pi}{2}$	4	$8k$	$8k$	$C_2 \times C_2 \times C_2$	$i(k)$
$\mathcal{Q}^k$, $k \geq 4$	$\pi-\delta$	$\frac{(k-1)\pi}{2k-1}-\delta$	$\frac{\pi}{2k-1}$	δ^4_k	$\frac{\pi}{2}$	4	$14k$	$14k$	V	$4k-2$
$\mathcal{R}^k$, $k \geq 6$	α^2_k	$\frac{\pi}{2}-\delta$	$\frac{\pi}{k}$	$\pi-\alpha$	$\frac{\pi}{2}$	4	$4k$	$4k$	$C_2 \times D_k$	4
$\mathcal{S}^k$, $k \geq 7$	$\pi-\delta$	$\frac{(k-1)\pi}{2k}-\delta$	$\frac{\pi}{k}$	δ^5_k	$\frac{\pi}{2}$	4	$8k$	$8k$	D_{2k}	4

Table 1: Combinatorial structure of the dihedral f-tilings of S^2 by scalene triangles T and isosceles triangles T' performed by the lower side of T and the longest side of T' in the case of adjacency II.

3 Proof of Theorem 2.1

In order to better understand the structure of each tiling and due to the complexity of a global planar representation, in the following proof some f-tilings τ are illustrated only by a fundamental region F that generates τ by successive reflections and rotations of F. Comparing the fundamental region F with its associated f-tiling τ (in Figure 4), it becomes clear how it is generated. In two of the situations (tilings Q^k and S^k), instead of a fundamental region, we illustrate planar representations that correspond to a half of the f-tilings.

In the case of adjacency II, any element of $\Omega\,(T, T')$ has at least two cells congruent to T and T', respectively, such that they are in adjacent positions and in one and only one of the situations illustrated in Figure 2. After certain initial assumptions are made, it is usually possible to deduce sequentially the nature and orientation of most of the other tiles. Eventually, either a complete tiling or an impossible configuration proving that the hypothetical tiling fails to exist is reached. In the diagrams that follow, the order in which these deductions can be made is indicated by the numbering of the tiles. For $j \geq 2$, the location of tiling j can be deduced directly from the configurations of tiles $(1, 2, \ldots, j-1)$ and from the hypothesis that the configuration is part of a complete tiling, except where otherwise indicated.

Observe that we have $\varepsilon > \frac{\pi}{3}$ (since we are considering the case of adjacency II). Also, as $e = c$ and using spherical trigonometric formulas, we get

$$\frac{\cos\gamma + \cos\alpha\cos\beta}{\sin\alpha\sin\beta} = \frac{\cos\varepsilon + \cos^2\delta}{\sin^2\delta}. \tag{3.1}$$

Proof of Theorem 2.1. Suppose that any element of $\Omega\,(T, T')$ has at least two cells congruent, respectively, to T and T', such that they are in adjacent positions as illustrated in Figure 2-II.

With the labeling of Figure 5a, we have $\theta_1 \in \{\varepsilon, \delta\}$. It is easy to verify that θ_1 must be δ. In fact, if $\theta_1 = \varepsilon$, v_1 cannot have valency four (see side lengths), $\alpha + \varepsilon + \rho > \pi$,

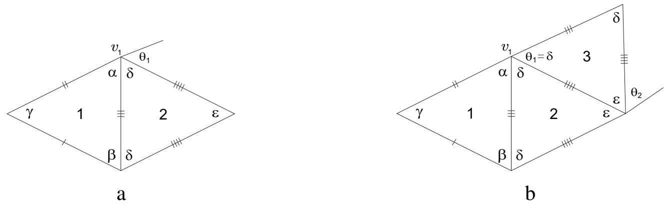

Figure 5: Local configurations.

$\forall\rho \in \{\alpha, \beta, \delta, \varepsilon\}$, and if $\alpha + \varepsilon + k\gamma = \pi$, $k \geq 1$, an incompatibility between sides cannot be avoided.

Now, at vertex v_1 (see Figure 5b) we must have

$$\alpha + \delta < \pi \quad \text{or} \quad \alpha + \delta = \pi.$$

1. Suppose firstly that $\alpha + \delta < \pi$. If $\theta_2 = \delta$ and $\varepsilon + \delta = \pi$ (Figure 6a), we reach a contradiction at vertex v_2, as $\varepsilon + \beta + \rho > \pi$, for all $\rho \in \{\alpha, \beta, \gamma, \delta, \varepsilon\}$. In fact, taking into account the side lengths, v_2 cannot have valency four and also observe that $\varepsilon + \beta + \rho_1 \geq \alpha + \beta + \gamma$, $\rho_1 \in \{\alpha, \beta, \gamma\}$, and $\varepsilon + \beta + \rho_2 > \varepsilon + \delta = \pi$, $\rho_2 \in \{\delta, \varepsilon\}$.

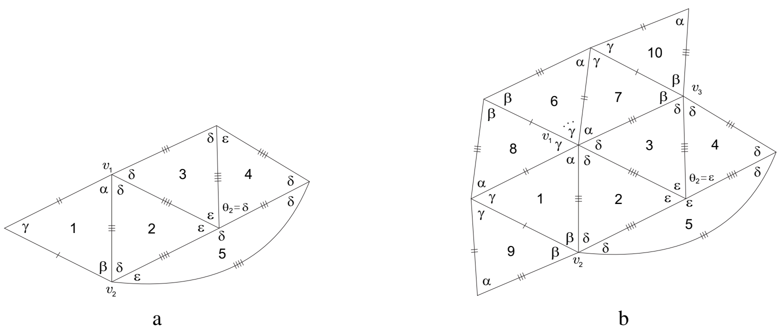

Figure 6: Local configurations.

On the other hand, if $\theta_2 = \delta$ and $\varepsilon + \delta < \pi$, we must have $\varepsilon + \delta + \rho \leq \pi$, for some $\rho \in \{\alpha, \beta, \gamma\}$. If $\rho = \alpha$, we get $\varepsilon > \delta > \alpha > \beta > \gamma$; but then $\varepsilon + \delta + \alpha > \alpha + \beta + \gamma > \pi$, which is not possible. If $\rho = \beta$, we obtain $\delta > \beta$ and $\alpha > \varepsilon$, which implies $\alpha + \delta + \bar{\rho} > \pi$, $\forall\bar{\rho}$, which is a contradiction. Finally, due to an incompatibility between sides, it is not possible to have $\varepsilon + \delta + k\gamma = \pi$, $k \geq 1$.

Therefore, $\theta_2 = \varepsilon$ and, due to the side lengths, we must have $\varepsilon + \varepsilon = \pi$, and obviously $\alpha > \delta$, with $\delta \in \left(\frac{\pi}{4}, \frac{\pi}{2}\right)$.

1.1 If $\alpha \geq \varepsilon$, at vertex v_1 (Figure 5b) we must have $\alpha + \delta + k\gamma = \pi$, with $k \geq 1$, and $\alpha > \beta > \delta > \gamma$. The last configuration extends to the one illustrated in Figure 6b.

If, at vertices v_2 and v_3, we have

(i) $\beta + \delta + \delta = \pi$, we reach a vertex surrounded by six angles δ, implying $\delta = \frac{\pi}{3} = \beta$, which is not possible as $\beta > \delta$;

(ii) $\beta + \delta + \beta = \pi$, we obtain the configuration illustrated in Figure 7a. Taking into account the edge lengths and the fact that $\beta > \delta > \frac{\pi}{4}$, at vertex v_4 we reach a contradiction.

Note that it is easy to conclude that is not possible to include angles γ in the previous sums.

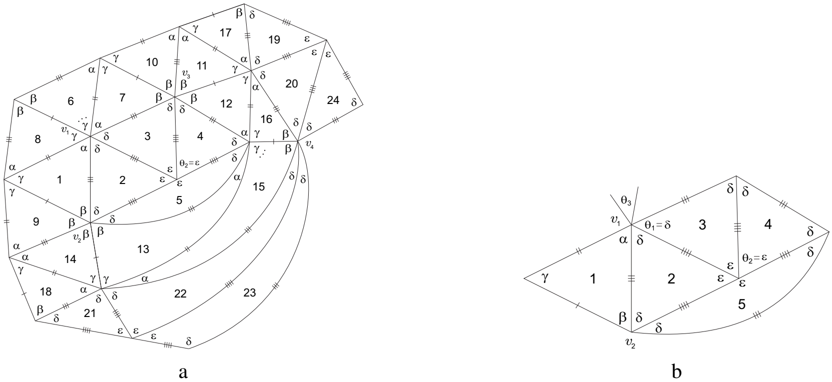

Figure 7: Local configurations.

1.2 Suppose now that $\alpha < \varepsilon$.

1.2.1 If $\delta \geq \gamma$, with the labeling of Figure 7b, we have $\theta_3 \in \{\delta, \gamma\}$. Additionally is important to note that $\varepsilon = \frac{\pi}{2} > \alpha > \beta > \delta \geq \gamma$, $\delta > \frac{\pi}{4}$ and $\beta + \gamma > \frac{\pi}{2}$.

If $\theta_3 = \delta$, we obtain the configuration of Figure 8a. Observe that θ_4 cannot be δ, as $\delta + \delta + \delta < \delta + \delta + \alpha = \pi$ and $\delta + \delta + \delta + \rho > \pi$, with $\rho \in \{\alpha, \beta, \delta, \varepsilon\}$; ρ_2 cannot be γ due to an incompatibility between sides. Moreover, θ_4 cannot be β, as $\delta + \delta + \beta < \pi$ and $\delta + \delta + \beta + \gamma > \pi$.

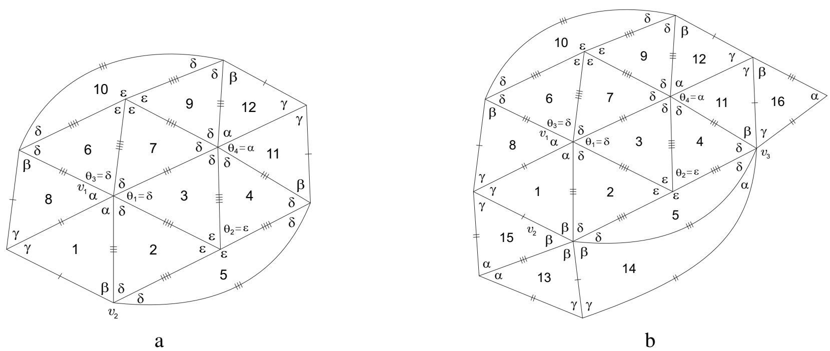

Figure 8: Local configurations.

Now, at vertex v_2 we have necessarily $\beta + \delta + \beta = \pi$ or $\beta + \delta + k\gamma = \pi$, with $k \geq 2$. These cases lead to the configurations illustrated in Figure 8b and Figure 9a, respectively. In both cases, at vertex v_3 we reach a contradiction. In fact, due to the edge and angles lengths there is no way to satisfy the angle-folding relation around this vertex.

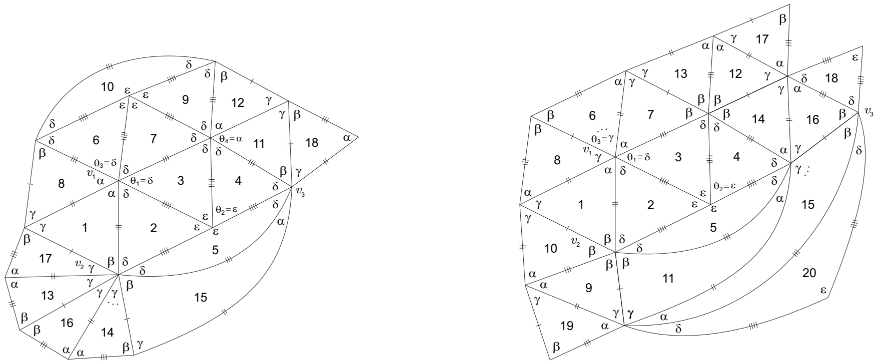

a b

Figure 9: Local configurations.

If $\theta_3 = \gamma$ (Figure 7b), at vertex v_2 we have necessarily $\beta+\delta+\beta = \pi$ or $\beta+\delta+\delta = \pi$. These cases lead to the configurations illustrated in Figure 9b and Figure 10a, respectively. In the first case, at vertex v_3 we have $\beta + \delta + \delta < \pi$ and $\beta + \delta + \delta + \rho > \pi$, for all $\rho \in \{\alpha, \beta, \gamma, \delta, \varepsilon\}$. In the last case, at vertex v_3 we also reach a contradiction, as $\delta = \frac{\pi}{3}$ implies $\beta = \frac{\pi}{3}$ and, due to the edge and angles lengths, it is not possible that this vertex has valency greater than three.

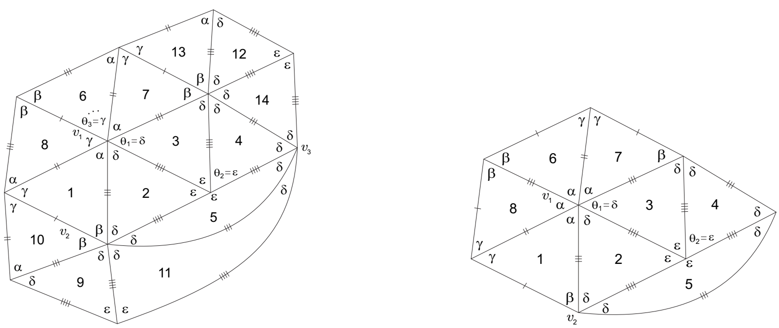

a b

Figure 10: Local configurations.

1.2.2 If $\delta < \gamma$, then $\varepsilon = \frac{\pi}{2} > \alpha > \beta > \gamma > \delta > \frac{\pi}{4}$. At vertex v_1 (Figure 7b) we must have one of the following situations:

(i) $\alpha+\delta+\alpha = \pi$; in this case (Figure 10b), there is no way to satisfy the angle-folding relation around vertex v_2.

(ii) $\alpha+\delta+\delta = \pi$; as we can observe in Figure 11a, an incompatibility between sides at vertex v_3 cannot be avoided.

(iii) $\alpha+\delta+\gamma = \pi$; in this case (Figure 11b), there is no way to satisfy the angle-folding relation around vertex v_4.

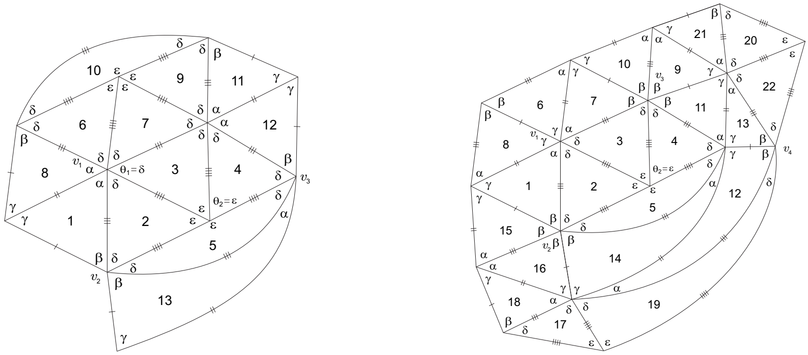

a b

Figure 11: Local configurations.

(iv) $\alpha+\delta+\beta=\pi$; in this situation, the last configuration extends to the one illustrated in Figure 12a. Now, at vertex v_4 we have necessarily $\gamma+\gamma+\rho=\pi$, with $\rho\in\{\alpha,\beta,\gamma\}$. It is easy to verify that the two first cases lead to impossibilities. The last case ($\rho=\gamma$) leads to a continuous family of f-tilings formed by 72 tiles. Due to the large dimension of the corresponding planar representation, we only illustrate its eighth fundamental region in Figure 12b.

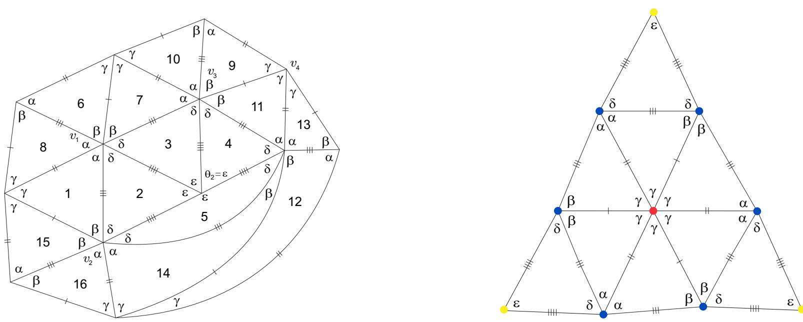

a b A eighth fundamental region of $\mathcal{L}_\beta$

Figure 12: Local configurations.

We denote this continuous family of f-tilings by $\mathcal{L}_\beta$, where

$$\alpha+\delta+\beta=\pi, \quad 2\varepsilon=\pi \quad \mathit{and} \quad 3\gamma=\pi.$$

Using Equation (3.1), we get

$$\sin^2(\alpha+\beta)\,(1+2\cos(\alpha-\beta)) = 2\sin\alpha\sin\beta, \quad \text{with} \quad \frac{\pi}{3}<\beta<\arccos\frac{\sqrt{6}}{6}.$$

3D representations of $\mathcal{L}_\beta$ are illustrated in Figure 4a.

2. Suppose now that $\alpha + \delta = \pi$. We have $\alpha > \delta$ and $\alpha > \frac{\pi}{2}$. In fact, if $\alpha \leq \delta$, we would have $\varepsilon > \delta \geq \alpha > \beta > \gamma$, with $\delta \geq \frac{\pi}{2}$, and consequently $\varepsilon + \theta_2 > \pi$, $\theta_2 \in \{\varepsilon, \delta\}$.

2.1 If $\theta_2 = \delta$ (Figure 5b), then it is a straightforward exercise to prove that $\gamma = \frac{\pi}{k}$, for some $k \geq 4$, and the complete planar representation derives uniquely as illustrated in Figure 13.

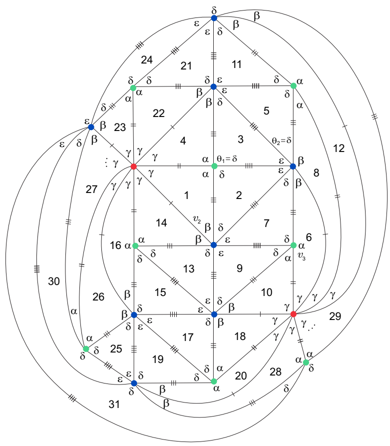

Figure 13: Planar representation of $\mathcal{D}_\varepsilon^k$, $k \geq 4$.

This family of f-tilings is denoted by $\mathcal{D}_\varepsilon^k$, where $\alpha + \delta = \pi$, $\delta + \beta + \varepsilon = \pi$ and $k\gamma = \pi$, with $k \geq 4$. Using (3.1), we get

$$\delta = \delta_k(\varepsilon) = \arctan \frac{2 \sin \varepsilon \cos^2 \frac{\varepsilon}{2}}{\cos \frac{\pi}{k} - \cos^2 \varepsilon}, \quad k \geq 4,$$

with $\varepsilon \in \left(\varepsilon_{\min}, \frac{(k-1)\pi}{k}\right)$, where $\varepsilon_{\min} = \arccos \frac{\sqrt{1+8\cos\frac{\pi}{k}}-1}{4}$. 3D representations of $\mathcal{D}_\varepsilon^4$ and $\mathcal{D}_\varepsilon^5$ are given in Figures 4c – 4d.

2.2 If $\theta_2 = \varepsilon$, we have $\beta \geq \delta$ or $\beta < \delta$.

2.2.1 If $\beta \geq \delta$, we have $\alpha > \frac{\pi}{2} = \varepsilon > \delta > \frac{\pi}{4}$ and the last configuration extends to the one illustrated in Figure 14a. Now, we have $\theta_3 \in \{\beta, \delta, \gamma\}$.

2.2.1.1 If $\theta_3 = \beta$, at vertex v_2 we must have $\delta + \beta + \beta + k\gamma = \pi$, with $k \geq 0$. It is easy to verify that k has to be zero, giving rise to the configuration of Figure 14b. At vertex v_3 we obtain $\alpha + \bar{k}\gamma = \pi$, with $\bar{k} \geq 2$. Taking into account Equation (3.1) and the relations between angles, we get $2\cos\frac{\delta}{k} = \cos\delta \csc\frac{\delta}{2}$. Consequently, we obtain $\sin\delta \leq \cos\delta$ and $\delta \leq \frac{\pi}{4}$, which is not possible.

2.2.1.2 If $\theta_3 = \delta$, at vertex v_2 we have $\delta + \beta + \delta + k\gamma = \pi$, with $k \geq 0$. It is a straightforward exercise to show that (i) if $k = 0$, although a complete configuration is achieved, it leads to $\beta = \gamma = \frac{\pi}{3}$, which is not possible; (ii) if $k = 1$, again a complete configuration is achieved, with $\delta = \frac{\pi}{3} = \beta + \gamma$, which is a contradiction; (iii) the case $k > 1$ leads to an incompatibility between sides.

2.2.1.3 If $\theta_3 = \gamma$, at vertex v_2 we must have one of the following situations:

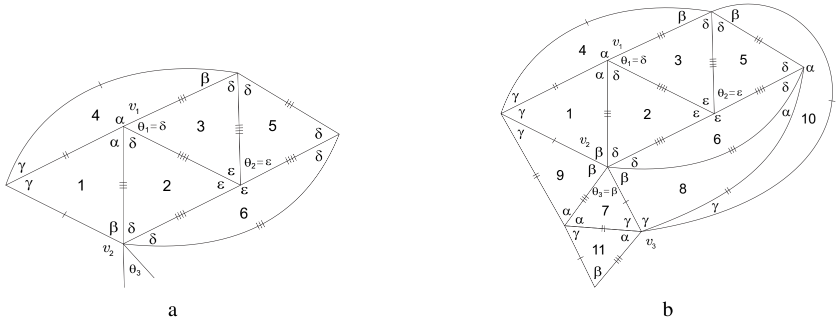

Figure 14: Local configurations.

(i) $\beta+\delta+k\gamma=\pi$, $k\geq 1$; the case $k>1$ leads to $\delta=\beta=\frac{\pi}{3}$, which is not possible, and so $k=1$. In this case we obtain the planar representation of Figure 15. We denote this family of f-tilings by $\mathcal{M}_\gamma$, where $\alpha+\delta=\pi$, $\beta+\delta+\gamma=\pi$ and $\gamma\in\left(\frac{\pi}{4},\frac{\pi}{3}\right)$. Using Equation (3.1), we get $\delta=\gamma$.

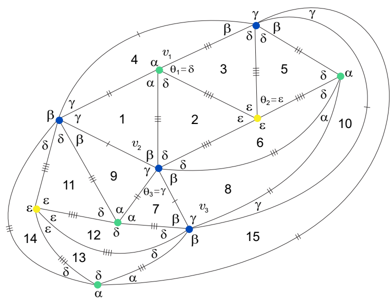

Figure 15: Planar representation of $\mathcal{M}_\gamma$.

3D representations of $\mathcal{M}_\gamma$, $\gamma\in\left(\frac{\pi}{4},\frac{\pi}{3}\right)$, are illustrated in Figure 4b.

(ii) $\beta+\delta+\beta+k\gamma=\pi$, $k\geq 1$; as we can observe in Figure 16a, we reach an impossibility as there is no way to complete the sum of alternate angles around vertex v_3.

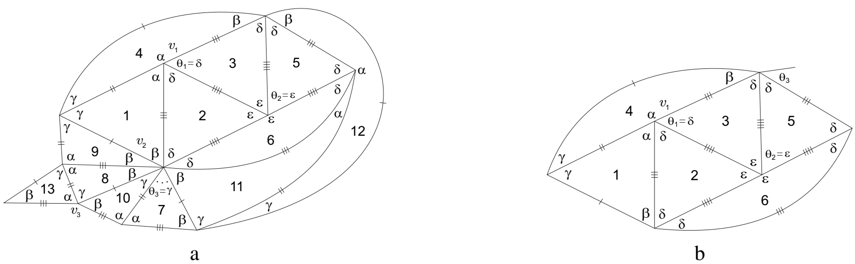

Figure 16: Local configurations.

(iii) $\beta+\delta+\delta+k\gamma=\pi$, $k\geq 1$; in this case there is no way to satisfy the angle-folding relation around vertex v_2.

2.2.2 If $\beta<\delta$ (Figure 5b), it is easy to conclude that $\alpha>\frac{\pi}{2}=\varepsilon>\delta>\beta>\gamma$. Now, with the labeling of Figure 16b we have $\theta_3\in\{\delta,\beta\}$.

2.2.2.1 If $\theta_3=\delta$, we obtain the configuration illustrated in Figure 17a. Note that θ_4 cannot be ε, otherwise there is no way to satisfy the angle-folding relation around vertex v_2. Also, θ_5 cannot be ε, as it implies $\theta_6=\alpha$. Now, at vertex v_3, we have necessarily $3\delta+\beta=\pi$. In fact, if $3\delta=\pi$, at vertex v_2 we obtain $\delta+\delta+\beta<\pi$ and $\delta+\delta+\beta+\rho>\pi$, $\rho\in\{\beta,\gamma\}$, as $\beta+\gamma>\delta$. Then, the last configuration extends uniquely to a complete

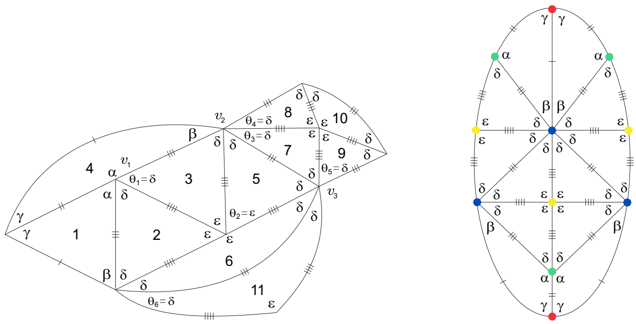

a

b A kth fundamental region of $\mathcal{N}^k$, $k\geq 6$.

Figure 17: Local configurations.

planar representation formed by $12k$ tiles. Due to its large dimension, we only illustrate the kth fundamental region in Figure 17b. As $\beta>\gamma$, using Equation (3.1), we must have $k\gamma=\pi$, with $k\geq 6$. We denote this family of f-tilings by $\mathcal{N}^k$, where $\alpha+\delta=\pi$, $3\delta+\beta=\pi$ and $k\gamma=\pi$, $k\geq 6$. Moreover,

$$\delta=\delta_k=\arccos\sqrt{\frac{1}{2}\cos\frac{\pi}{k}},\quad k\geq 6.$$

3D representations of $\mathcal{N}^k$, for $k=6,7$, are illustrated in Figures 4e – 4f.

2.2.2.2 If $\theta_3=\beta$, we obtain the configuration of Figure 18a.

It is a straightforward exercise to prove that if vertex v_2 has valency six, we obtain $\alpha+k\gamma=\pi$, $k\geq 2$, or $\beta+\delta+\gamma=\pi$, and in either cases Equation (3.1) has no solution. Moreover, this equation also has no solution if there is a vertex with a sum of alternate angles of the form $\beta+\delta+\delta=\pi$. Now, we consider separately the cases $\theta_4=\theta_5=\gamma$, $\theta_4=\theta_5=\beta$, and $\theta_4=\beta$ and $\theta_5=\gamma$.

2.2.2.2.1 If $\theta_4=\theta_5=\gamma$, vertex v_2 must have valency greater than eight. In fact, valency eight implies the existence of a vertex with a sum of alternate angles of the form $\beta+\delta+\delta=\pi$.

Now, with the labeling of Figure 18b, if v_2 has valency greater or equal to ten and

- there is an additional angle β in the sum of alternate angles (note that is not possible to have an additional angle δ, as $2\delta+2(\beta+\gamma)>\pi$), the last configuration extends

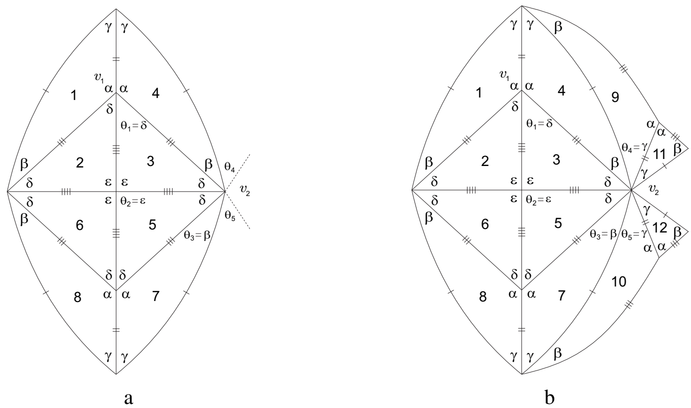

Figure 18: Local configurations.

to the one illustrated in Figure 19a and there is no way to satisfy the angle-folding relation around vertex v_3.

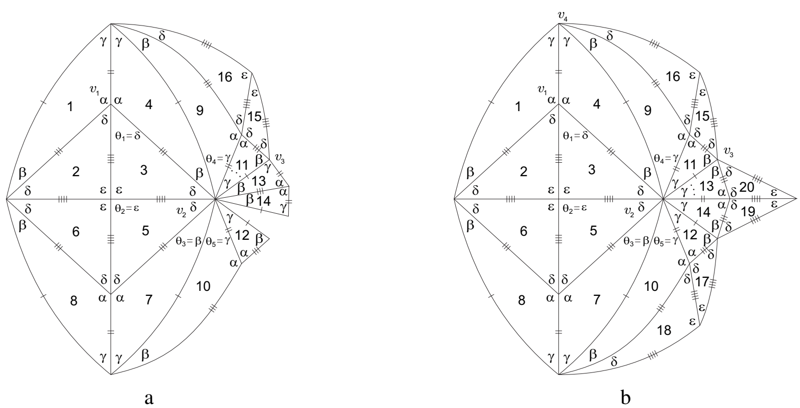

Figure 19: Local configurations.

- $\beta + \delta + k\gamma = \pi$, with $k \geq 3$, we obtain the configuration illustrated in Figure 19b. At vertex v_3 we must have one of the following situations:
  - (i) $\beta + \delta + \varepsilon = \pi$; this condition leads to a sum of alternate angles at vertex v_4 containing $\varepsilon + \delta + \beta + \gamma > \pi$, which is not possible;
  - (ii) $\beta + \delta + \delta + \beta = \pi$; in this case we obtain a complete planar representation formed by $16k$ tiles. Due to its dimension, we only illustrate one octant of the sphere (fundamental region) in Figure 20. Observe that one of the hemispheres is obtained from the other through a 90 degree rotation. Note that if $\theta_6 = \delta$, we would obtain $\beta + 3\delta = \pi$ and consequently no solution would exist for Equation (3.1). We have $\delta = \arctan\left(\sec\frac{\pi}{2k}\right)$, $\beta = \frac{\pi}{2} - \delta$, $\gamma = \frac{\pi}{2k}$, $\alpha =$

$\pi - \delta$, $\varepsilon = \frac{\pi}{2}$ and $k \geq 3$. We denote this f-tiling by $\mathcal{P}^k$, $k \geq 3$, whose 3D representations, for $k = 3, 4$, are presented in Figures 4g – 4h.

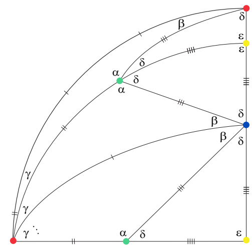

Figure 20: A eighth fundamental region of $\mathcal{P}^k$, $k \geq 3$.

(iii) $\beta + \delta + \delta + \beta + \beta = \pi$; in this case we have necessarily $k \geq 4$ and it gives rise to a sum of alternate angles of the form $\alpha + \bar{k}\gamma = \pi$, with $\bar{k} \geq 2$. Due to the angles relations, we have $\bar{k} = 2$. Nevertheless, under these conditions, Equation (3.1) has no solution.

(iv) $\beta + \delta + \delta + \beta + \gamma = \pi$; in this case we also have $k \geq 4$ and we obtain a complete planar representation formed by $28k$ tiles. Due to its large dimension, we only illustrate one hemisphere in Figure 21. The other hemisphere is obtained through a 180 degree rotation along the x axis and a reflection. We have $\delta = \arctan\left(\sin\frac{(k-1)\pi}{2k-1}\sec\frac{\pi}{2k-1}\right)$, $\beta = \frac{(k-1)\pi}{2k-1} - \delta$, $\gamma = \frac{\pi}{2k-1}$, $\alpha = \pi - \delta$ and $\varepsilon = \frac{\pi}{2}$. We denote this f-tiling by $\mathcal{Q}^k$, $k \geq 4$, whose 3D representations, for $k = 4, 5$, are presented in Figures 4i – 4j.

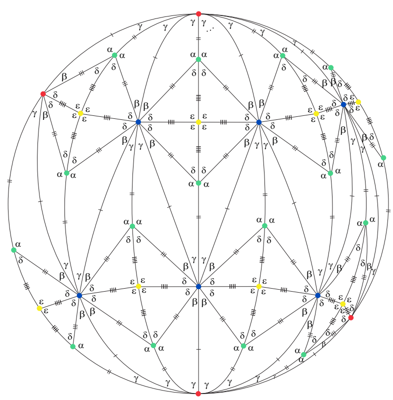

Figure 21: One hemisphere of $\mathcal{Q}^k$, $k \geq 4$.

(v) $\beta + \delta + \delta + \delta = \pi$; under this condition, it is easy to verify that we achieve at vertex v_4 (see Figure 19b) a sum of alternate angles containing $\delta + \delta + \beta + \gamma$, but $\delta + \delta + \beta + \gamma < \delta + \delta + \beta + \delta = \pi$ and $\delta + \delta + \beta + \gamma + \rho > \pi$, for all $\rho \in \{\alpha, \beta, \delta, \varepsilon\}$.

2.2.2.2.2 If $\theta_4 = \theta_5 = \beta$ (Figure 18a), it is easy to observe that vertex v_2 cannot be surrounded by six consecutive angles β, as we obtain a vertex with a sum of alternate angles of the form $\alpha + \gamma + \rho$, with $\rho \in \{\alpha, \beta, \delta\}$, which is not possible. Moreover, it is not possible to have angles γ surrounding v_2, as it gives rise to a vertex with a sum of alternate angles containing α and β. Taking into account these restrictions and analyzing the angles relations and side lengths, at vertex v_2 we must have one of the following cases:

(i) $\beta + \delta + \beta + \delta = \pi$; in this case we obtain the configuration illustrated in Figure 22a.

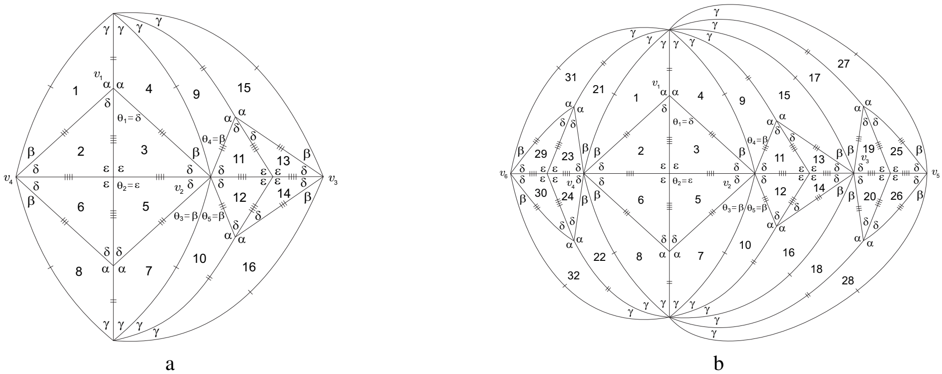

Figure 22: Local configurations.

Given the sums of alternate angles $S_1 : \beta + \delta + \beta + \delta = \pi$ and $S_2 : \beta + \delta + k\gamma = \pi$, $k \geq 3$, it is a straightforward exercise to prove that at vertices v_3 and v_4 we must have only S_1 or a combination of S_1 and S_2 (note that we have symmetry, so order does not matter). If we have a combination of S_1 and S_2, we obtain a complete representation of f-tiling $\mathcal{P}^k$, $k \geq 3$, previously achieved. On the other hand, if we have only S_1, the last configuration extends to the one illustrated in Figure 22b. At vertices v_5 and v_6 we must have only S_1 or S_2. In the last case, as before we obtain the f-tiling $\mathcal{P}^k$, with $k \geq 4$. If S_1 is the sum of alternate angles at vertices v_5 and v_6, then we obtain a complete representation formed by $8k$ tiles. A fundamental region is illustrated in Figure 23. For each $k \geq 6$, we have $\alpha = 2\arctan\left(\cos\frac{\pi}{k} + \sqrt{1 + \cos^2\frac{\pi}{k}}\right)$, $\beta = \frac{\pi}{2} - \delta$, $\gamma = \frac{\pi}{k}$, $\delta = \pi - \alpha$ and $\varepsilon = \frac{\pi}{2}$. We denote this f-tiling by $\mathcal{R}^k$, $k \geq 6$, whose 3D representations, for $k = 6, 7$, are presented in Figures 4k – 4l.

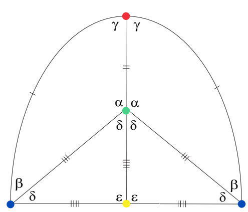

Figure 23: A $2k$th fundamental region of $\mathcal{R}^k$, $k \geq 6$.

(ii) $\beta + \delta + \beta + \delta + \beta = \pi$; this case leads to the following additional relations between angles: $\alpha + \gamma + \gamma = \pi$ and $k\gamma = \pi$, with $k \geq 8$. Nevertheless, under these conditions, (3.1) has no solution.

2.2.2.2.3 If $\theta_4 = \beta$ and $\theta_5 = \gamma$ (Figure 18a), it is easy to observe that vertex v_2 cannot be surrounded by the sequence $(\ldots, \beta, \beta, \gamma, \gamma, \ldots)$, as we achieve a vertex with a sum of alternate angles containing $\alpha + \beta$, which is not possible as $\alpha + \beta + \rho > \pi$, for all ρ. As the sum of alternate angles surrounding v_2 must contain at least one angle γ, taking into account the previous restriction and analyzing angles relations and side lengths, at vertex v_2 we have necessarily $\beta + \delta + \beta + \delta + \gamma = \pi$, as illustrated in Figure 24.

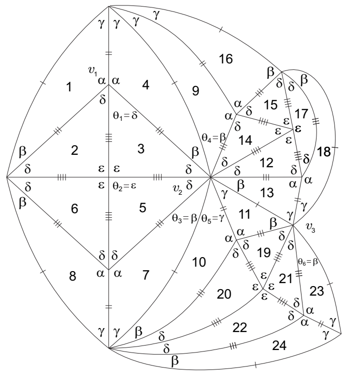

Figure 24: Local configuration.

Note that θ_6 must be β (tile 23), as $\theta_6 = \delta$ immediately leads to an impossibility. It is a straightforward exercise to verify that at vertex v_3 we must have $\beta + \delta + k\gamma = \pi$, with $k \geq 4$, or $\beta + \delta + \beta + \delta + \gamma = \pi$. In the first case, analyzing the symmetry of the figure and all possible combinations of angles surrounding specific vertices, we obtain the f-tiling $\mathcal{Q}^k$, $k \geq 4$, formerly achieved. In the last case, beside this family of f-tilings, we also obtain a complete planar representation formed by $16k$ tiles. Due to its dimension, we only illustrate one hemisphere in Figure 25. the other hemisphere is obtained through a 180 degree rotation along the x axis and a reflection.

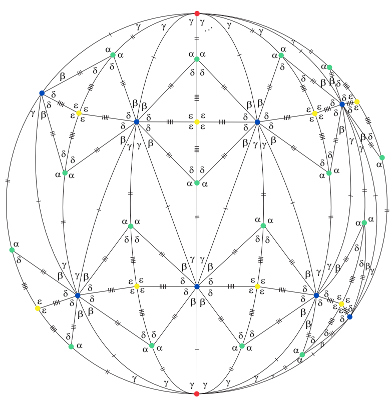

Figure 25: One hemisphere of $\mathcal{S}^k$, $k \geq 7$.

We have $\delta = \arctan\left(\sin \frac{(k-1)\pi}{2k} \sec \frac{\pi}{2k}\right)$, $\beta = \frac{(k-1)\pi}{2k} - \delta$, $\gamma = \frac{\pi}{k}$, $\alpha = \pi - \delta$ and

$\varepsilon = \frac{\pi}{2}$. We denote this f-tiling by $\mathcal{S}^k$, $k \geq 7$, whose 3D representations, for $k = 7, 8$, are presented in Figures 4m – 4n. □

ORCID iDs

Catarina P. Avelino https://orcid.org/ 0000-0003-4335-0185
Altino F. Santos https://orcid.org/ 0000-0002-8638-4644

References

[1] C. P. Avelino and A. F. Santos, S^2 coverings by isosceles and scalene triangles—adjacency case I, *Ars Math. Contemp.* **16** (2019), 419–443, doi:10.26493/1855-3974.1401.7d9.

[2] A. M. R. Azevédo Breda, A class of tilings of S^2, *Geom. Dedicata* **44** (1992), 241–253, doi:10.1007/bf00181393.

[3] R. J. M. Dawson, Tilings of the sphere with isosceles triangles, *Discrete Comput. Geom.* **30** (2003), 467–487, doi:10.1007/s00454-003-2846-4.

[4] R. J. M. Dawson and B. Doyle, Tilings of the sphere with right triangles. I. The asymptotically right families, *Electron. J. Comb.* **13** (2006), Research Paper 48, 31, doi:10.37236/1074.

[5] R. J. M. Dawson and B. Doyle, Tilings of the sphere with right triangles. II. The $(1, 3, 2), (0, 2, n)$ subfamily, *Electron. J. Comb.* **13** (2006), Research Paper 49, 22, doi:10.37236/1075.

[6] A. M. R. d'Azevedo Breda and P. S. Ribeiro, Spherical f-tilings by two non-congruent classes of isosceles triangles—I, *Math. Commun.* **17** (2012), 127–149.

[7] A. M. R. d'Azevedo Breda and P. S. Ribeiro, Spherical f-tilings by two non-congruent classes of isosceles triangles—II, *Acta Math. Sin. Engl. Ser.* **30** (2014), 1435–1464, doi:10.1007/s10114-014-3302-5.

[8] A. M. R. d'Azevedo Breda and A. F. Santos, Dihedral f-tilings of the sphere by spherical triangles and equiangular well-centered quadrangles, *Beiträge Algebra Geom.* **45** (2004), 447–461.

[9] A. M. R. d'Azevedo Breda and A. F. Santos, Symmetry groups of a class of spherical foldings tilings, *Appl. Math. Inf. Sci.* **3** (2009), 123–134.

[10] S. A. Robertson, Isometric folding of Riemannian manifolds, *Proc. Roy. Soc. Edinburgh Sect. A* **79** (1977/78), 275–284, doi:10.1017/S0308210500019788.

[11] Y. Ueno and Y. Agaoka, Classification of tilings of the 2-dimensional sphere by congruent triangles, *Hiroshima Math. J.* **32** (2002), 463–540, `http://projecteuclid.org/euclid.hmj/1151007492`.